Science Advances
AAAS

Supplementary Materials for

Personalized chordoma organoids for drug discovery studies

Ahmad Al Shihabi, Ardalan Davarifar, Huyen Thi Lam Nguyen, Nasrin Tavanaie, Scott D. Nelson, Jane Yanagawa, Noah Federman, Nicholas Bernthal, Francis Hornicek, Alice Soragni*

*Corresponding author. Email: alices@mednet.ucla.edu

Published 16 February 2022, *Sci. Adv.* **8**, eabl3674 (2022)
DOI: 10.1126/sciadv.abl3674

The PDF file includes:

Other Supplementary Material for this manuscript includes the following:

Supplementary Text

CHORD001 was diagnosed as a conventional type chordoma of the thoracic spine in a 64-year-old woman (**Table 1**). The primary mass was 1.5 cm in greatest dimension, moderately differentiated, with no necrosis or lymphovascular invasion. Histologic staining showed mixed staining for brachyury with a subset of the cells staining negative for this marker (**Fig. 2**). The patient remains disease free at 37 months of follow up.

CHORD002 is a rare case of aggressive, metastatic conventional type chordoma of the sacrum diagnosed in a 27-year-old male (**Table 1**). The patient had a primary resection of an 8 cm mass with conventional histopathology and no lymphovascular invasion or necrosis. Next-generation sequencing analysis showed that the tumor had a low microsatellite instability (MSI), with loss of CDKN2A and CDKN2B. Only 6 months after surgical resection, the patient presented with metastatic recurrence to the lungs, spine, and pubic bone. A first sample was obtained from a biopsy of the pubic bone metastasis (CHORD002a) and confirmed to be conventional chordoma by pathologic morphology. The patient was treated with nivolumab, a PD-1 targeting monoclonal antibody (34), in combination with the mTOR inhibitor nab-rapamycin (34) as part of a clinical trial and started on a monoclonal antibody targeting RANKL, denosumab(34). Treatment was discontinued after 3 cycles and followed by a combination regimen with trabectedin, an alkaloid that binds to DNA to arrest transcription(34), nivolumab and an oncolytic herpes virus derivative (34) as part of a different trial.

We then obtained a second sample from the resection of a vertebral metastasis (CHORD002b). The mass measured 1 cm in the largest dimension and was positive for INI1 and Ki-67 as per the pathologist's assessment. Most of the tumor was viable, with only 15% necrosis. The patient subsequently received one cycle of nivolumab, followed by a trial of DeltaRex-G, a retroviral vector encoding a cyclin G1 inhibitor (35), followed by cetuximab, a monoclonal antibody targeting EGFR (34) in combination with nivolumab in the setting of a clinical trial.

We procured a third tissue sample, CHORD002c, from a resection of metastatic lesions in the cervical and thoracic spine. This tumor was again classified as a conventional type chordoma with positive Ki-67 (35%), retained/positive INI1, and positive brachyury on the pathology report. Whole exome NGS of the metastatic thoracic sample showed that loss of CDKN2A and CDKN2B was maintained, and the tumor had low mutational burden (TMB, 0.5 m/Mb). The patient subsequently received cyclophosphamide (an alkylating chemotherapeutic nitrogen mustard(34), palbociclib (a small molecule inhibitor of CDK4/6(34)), and cisplatin (a platinum derivative that binds DNA)(34).

CHORD003 is a 61-year-old woman diagnosed with a not-otherwise-specified (NOS) chordoma of the sacrum (**Table 1**). At the time of resection, the mass was 8 cm in size, well-differentiated, with rare mitoses, and areas of focal necrosis. There was a first local recurrence 3 years post diagnosis in the right acetabulum. The mass was a low-grade conventional chordoma measuring 3 cm in size. We obtained a tissue sample from a second recurrence diagnosed 15 months later in the right acetabulum. The specimen measured 3.4 cm in size, from which we obtained a sample for our study (CHORD003, **Fig. 1**). Immunohistochemistry showed retained INI1 and negative PDL-1 in tumor cells as well as significant Ki-67 positivity as noted in the pathology report (**Fig. 2**). MRI of the sacrum approximately after 4 months of follow up showed residual disease in the acetabulum.

CHORD004 is a case of NOS chordoma of the lumbar spine in a 48-year-old male (**Table 1**). We obtained a specimen from the initial resection the mass affecting the L1-L3 vertebrae (CHORD004). The tumor was 6 cm by radiographic imaging and mildly necrotic (20%). The patient presented with a recurrence of the tumor in the lower thoracic spine as well as chest metastases after a 19-month follow up.

CHORD005 is a 73-year-old diagnosed with NOS chordoma of the sacrum (**Table 1**). The resected specimen measured 11 cm in the largest dimension, with negative margins and focal areas of necrosis. The patient has no evidence of recurrence after 21-month follow up.

Supplementary Figures

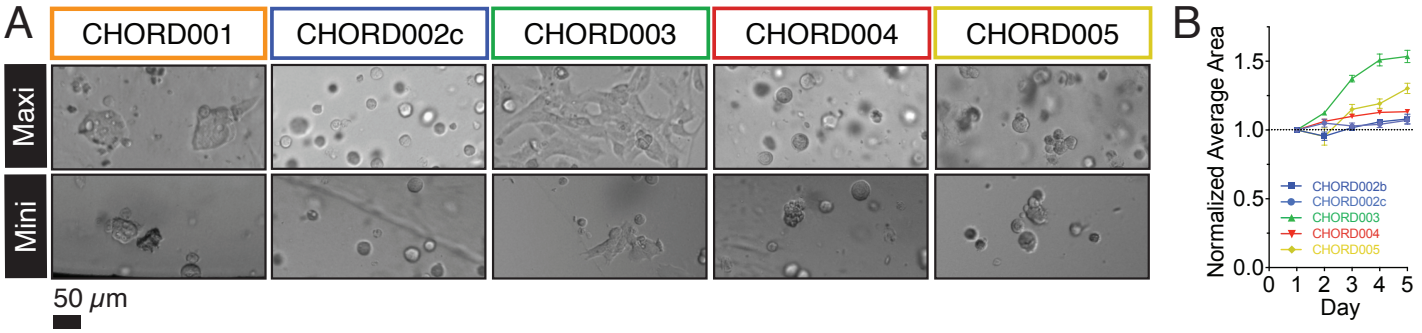

Supplementary Figure 1. Morphology and growth of chordoma PDOs. **(A)** Comparison of organoid morphology in mini- and maxi-ring cultures. Representative photos of PDOs were selected at day 5 of incubation. All samples displayed features that are characteristic of chordoma cells, and indistinguishable between the two formats. Scale bar 50 µm. **(B)** Chordoma PDO growth over time. A neural net was used for organoid detection and calculation of normalized average area over the 5 days. We selected images for neural net segmentation and detection of organoids from all our samples except for CHORD001 due to the absence of adequate images.

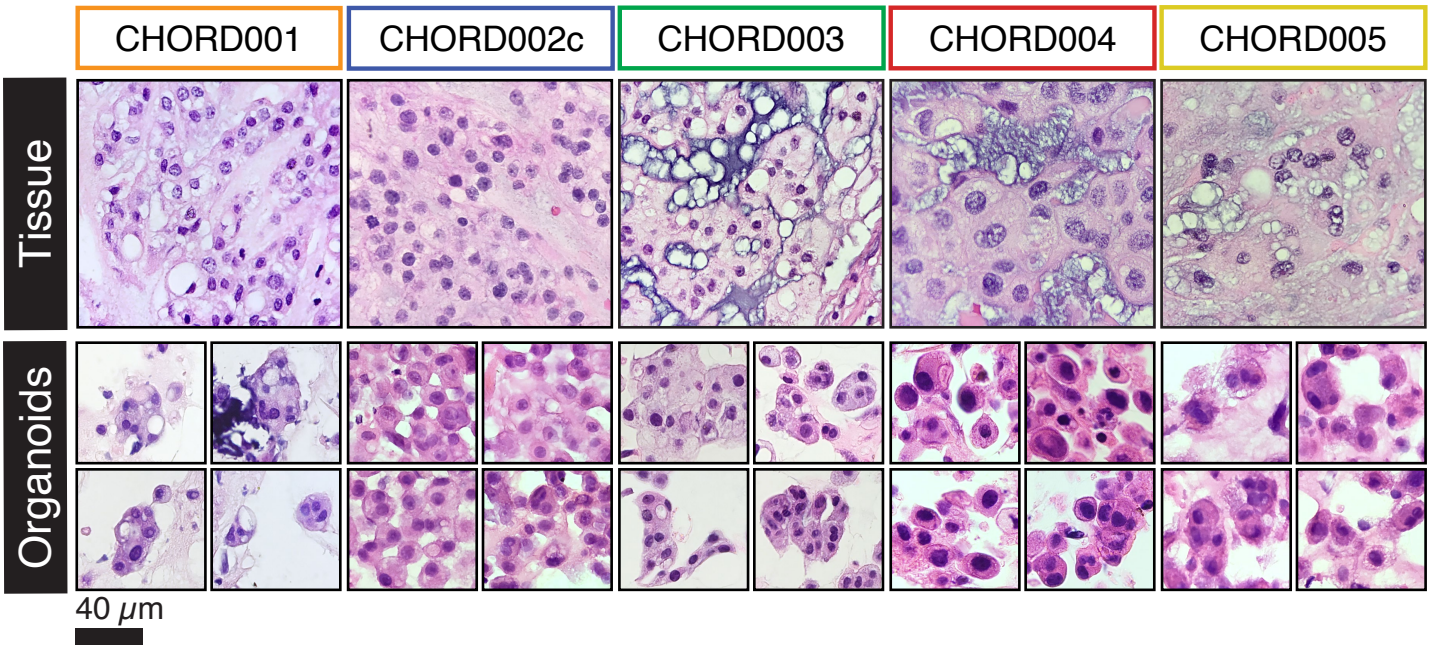

Supplementary Figure 2. Expanded field of view of tissue and organoid H&E staining. Wider field of view of the images shown in Figure 2 for tissue of CHORD001, CHORD003, CHORD004 and CHORD005 are shown, in addition to representative images for CHORD002c. Organoid images include wider views of some of the pictures shown in Figure 2 (CHORD001, CHORD003) as well as additional images for all samples, to further show that organoids recapitulate features of the parent tissue and display characteristic chordoma histology. Scale bar 40 µm.

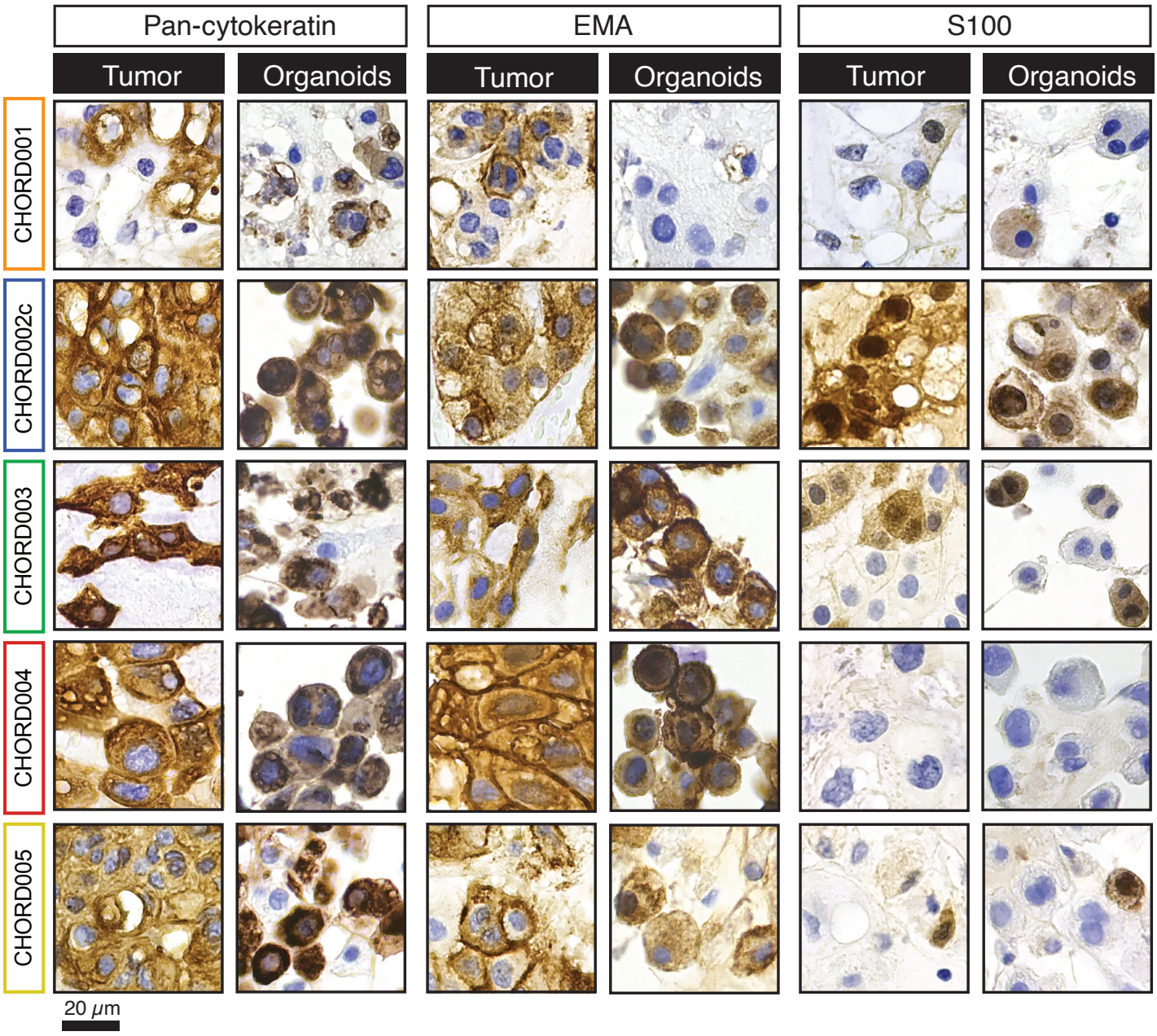

Supplementary Figure 3. Expanded immunohistochemistry panel performed on chordoma tissue and organoids. Pan-cytokeratin, EMA and S100 staining was perfomed on the indicated samples. Scale bar 20 μm.

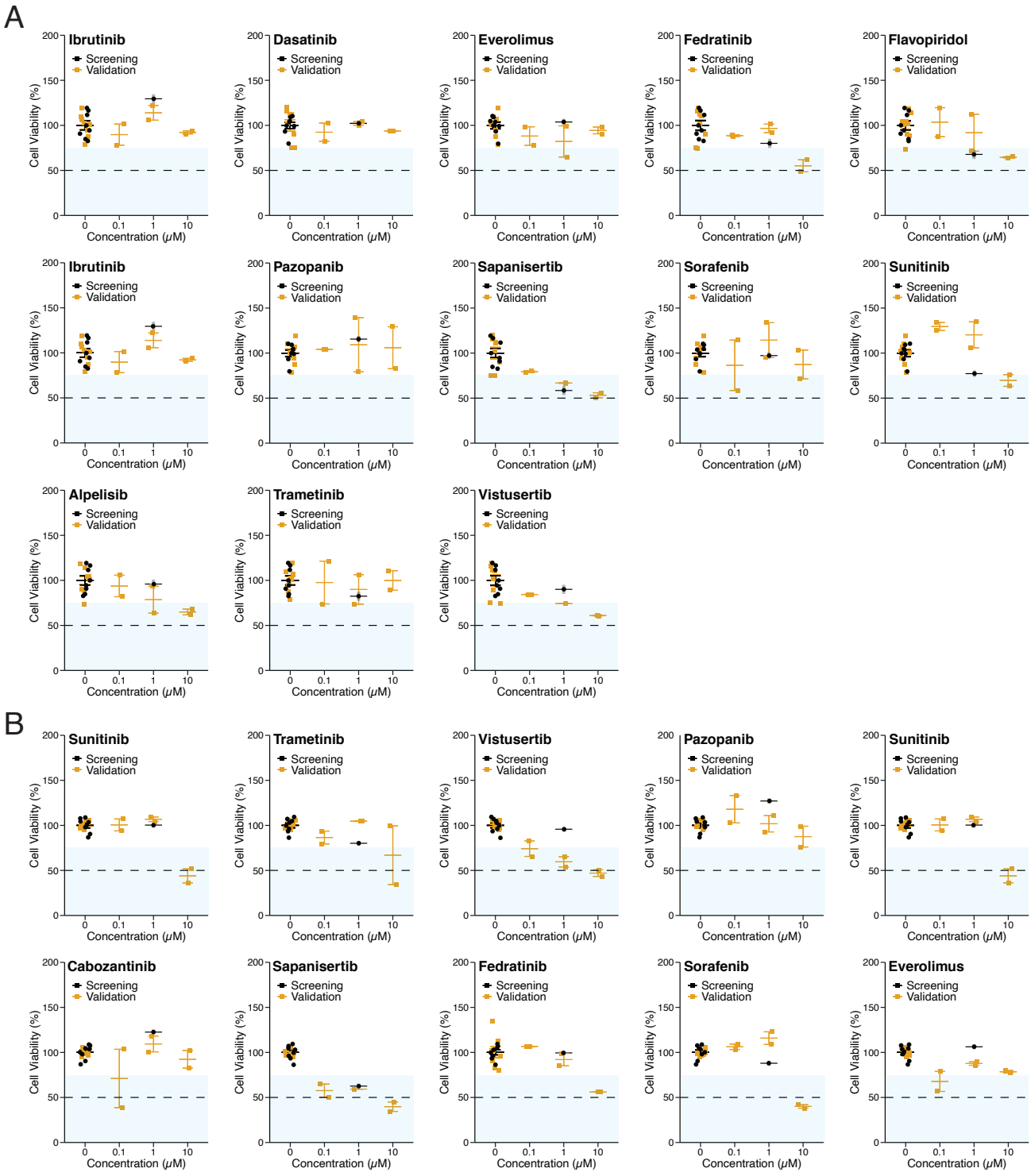

Supplementary Figure 4. Dose-response plots of drugs tested in both single concentration (1μM) discovery screening and in subsequent validation screening at multiple concentrations (0.1μM, 1μM, and 10μM) on samples CHORD002c **(A)** and CHORD005 **(B)**. Points represent individual wells, error bars show SEM. Discovery screening data is shown in black while validation screening values are in yellow.

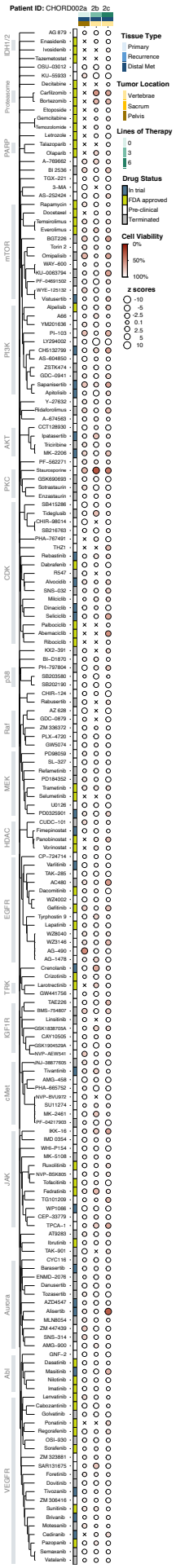

Supplementary Figure 5. Dot map showing the full drug screening results on all three samples obtained from patient CHORD002. The number of drugs tested on sample CHORD002a, CHORD002b, and CHORD002c is 155, 159 and 179 respectively, with X labeling drugs that were not screened. The size of each circle represents the Z score, with larger ones indicating a higher Z score value. The color of each point represents the normalized cell viability %. The drugs are clustered using the Jaccard distance based on common protein targets. Samples are ordered by date of acquisition. The covariates included show the type of tissue, anatomic site and the number of lines of treatment the patient was exposed to prior to procurement of sample.

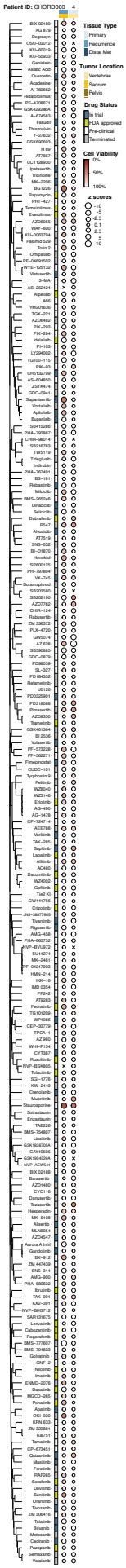

Supplementary Figure 6. Dot map of the complete drug screening results on samples CHORD003 and CHORD004. Number of drugs tested on sample CHORD003, and CHORD004 is 232 and 229 respectively, with X marking compounds not screened in one of the samples. The size of each circle represents the Z score, with larger ones indicating a higher Z score value. The color of each point represents the normalized cell viability %. The drugs are clustered using the Jaccard distance based on common protein targets. Covariates included represent the type of tissue, and anatomic location of each sample.

Supplementary Tables

Sample #	Number of Drugs Tested	% Drugs inducing 25% Cell Death*	% Drugs inducing 50% Cell Death*	% Drugs inducing 75% Cell Death*
CHORD001	140	7.1% (10/140)	0.7% (1/140)	0.0% (0/140)
CHORD002a	154	1.9% (3/154)	0.0% (0/154)	0.0% (0/154)
CHORD002b	165	8.5% (14/165)	1.2% (2/165)	0.0% (0/165)
CHORD002c	188	24.5% (46/188)	5.9% (11/188)	2.7% (5/188)
CHORD003	231	15.2% (35/231)	1.3% (3/231)	0.0% (0/231)
CHORD004	228	6.6% (15/228)	0.9% (2/228)	0.0% (0/228)
CHORD005	171	19.3% (33/171)	4.7% (8/171)	0.6% (1/171)

Supplementary Table 1. Summary of results of the high-throughput screening for all PDOs. For each sample, the number of total drugs that were tested, and the percentage of drugs inducing 25%, 50% and 75% are listed. *Excludes Staurosporine.

	CHORD001		CHORD002a		CHORD002b		CHORD002c		CHORD003		CHORD004		CHORD005	
Drug Name	Viability %	Z Score	Viability %	Z Score	Viability %	Z Score	Viability %	Z Score	Viability %	Z Score	Viability %	Z Score	Viability %	Z Score
Staurosporine	24.4	-26.9	71.3	-3.7	26.8	-7.5	44.3	-4.2	24.0	-5.5	37.8	-3.5	9.3	-11.5
BGT226	27.1	-26.1	79.3	-3.0	100.0	1.7	62.2	-2.7	40.4	-5.1	93.9	-0.4	58.9	-5.3
Sapanisertib	58.4	-14.9	76.7	-3.4	89.9	-1.5	64.0	-2.2	45.5	-4.7	91.2	-0.5	60.4	-8.7
Omipalisib	64.9	-12.6	70.2	-4.4	100.0	0.1	63.9	-2.5	100.0	1.2	100.0	2.0	54.8	-5.8
Fedratinib	100.0	5.3	91.9	-1.2	71.8	-4.1	91.1	-0.6	69.1	-2.6	79.6	-1.2	93.5	-0.4
Vistusertib	68.3	-11.4	100.0	0.2	100.0	0.9	79.5	-1.2	94.2	-0.5	86.8	-0.8	71.6	-7.2
Apitolisib	80.3	-7.1	100.0	0.4	100.0	4.2	85.7	-1.0	71.6	-2.4	100.0	1.2	75.1	-3.2
Gefitinib	100.0	4.4	82.1	-2.1	100.0	0.6	75.8	-2.4	100.0	1.2	100.0	2.0	55.5	-5.6
Sunitinib	99.4	-0.2	89.4	-1.3	90.1	-0.9	100.0	0.3	55.8	-2.7	100.0	0.3	100.0	1.2
Imatinib	100.0	5.9	100.0	0.8	100.0	0.8	100.0	0.3	73.3	-1.6	100.0	0.7	100.0	2.2

Supplementary Table 2. Summary of results of the high-throughput screening on a selected number of drugs. Viability and Z score are listed across all samples

Supplementary Movie

Supplementary Movie 1. Compiled images as shown in Figure 1.